β-Ga$_2$O$_3$ solar-blind deep-ultraviolet photodetector based on a four-terminal structure with or without Zener diodes

L. X. Qian,[1,2,a] X. Z. Liu,[1,2] T. Sheng,[1,2] W. L. Zhang,[1,2] Y. R. Li,[1,2] and P. T. Lai[3]

[1]*School of Microelectronics and Solid-State Electronics, University of Electronic Science and Technology of China, Chengdu 610054, China*
[2]*State Key Laboratory of Electronic Thin Films and Integrated Devices, University of Electronic Science and Technology of China, Chengdu 610054, China*
[3]*Department of Electrical and Electronic Engineering, The University of Hong Kong, Pokfulam Road, Hong Kong, Hong Kong*

A four-terminal photodetector was fabricated on the ($\bar{2}$01)-dominant *β*-Ga$_2$O$_3$ thin film which was deposited in a plasma-assisted molecular beam epitaxy system. The suitability of this film for solar-blind DUV detection was proved by its transmission spectra. Moreover, the device operating in a specific voltage-current mode can accurately detect the DUV radiation both qualitatively and quantitatively. Accordingly, a dark/photo voltage ratio of 15 was achieved, which is comparable to that of previously-reported *β*-Ga$_2$O$_3$ interdigital metal-semiconductor-metal photoconductor. More importantly, the aperture ratio of our proposed device exceeds 80%, nearly doubling that of the conventional interdigital metal-semiconductor-metal devices including photoconductor and Schottky-type photodiode, which can intensively benefit the detection efficiency. Furthermore, it was found the dark/photo voltage ratio was nearly trebled with the assistance of two Zener diodes, and further enhancement can be expected by increasing the operating current and/or adopting Zener diodes with smaller Zener voltage. Therefore, this work provides a promising alternative for solar-blind DUV detection. © *2016 Author(s). All article content, except where otherwise noted, is licensed under a Creative Commons Attribution (CC BY) license (http://creativecommons.org/licenses/by/4.0/).* [http://dx.doi.org/10.1063/1.4947137]

I. INTRODUCTION

Detectors which only sense radiations with wavelength shorter than 280 nm are usually classified as solar-blind deep-ultraviolet (DUV) photodetectors because there are only a few photons in this wavelength region reaching the Earth surface from the sun due to strong absorption by the stratospheric ozone layer.[1,2] Accordingly, this kind of photodetectors can accurately respond to a very weak signal even under sun or room illumination, providing an incomparable advantage especially for applications such as ozone-hole monitoring, flame detection and missile early warning.[3–5] At present, Si-based photodiode is the most commonly used in commercial applications due to its high compatibility with the mature silicon process.[6] Nevertheless, it is also sensitive to the infrared, visible and near-UV radiations due to the small bandgap (E_g) of Si (1.1 eV),[7,8] and accordingly expensive and cumbersome Woods optical filters have to be employed in solar-blind DUV detection system.[1,2] In this case, photodetectors based on wide-bandgap semiconductors are regarded as better alternatives. Among them, monoclinic Ga$_2$O$_3$ (*β*-Ga$_2$O$_3$) with an intrinsic E_g of 4.9 eV is naturally suitable for solar-blind DUV detection,[9,10] and so can avoid the alloying process in material growth for AlGaN[11,12] and ZnMgO.[13] As a result, β-Ga$_2$O$_3$ has attracted much attention in recent years, and its characteristics of solar-blind DUV detection have been demonstrated in various device structures.[14–17] Metal-semiconductor-metal (MSM) photoconductor based on *β*-Ga$_2$O$_3$ thin film is

---

[a]corresponding author electronic mail: lxqian@uestc.edu.cn

particularly promising due to its large photocurrent gain, high responsivity, easy integration with readout circuitry, etc. However, the detection characteristics could be degraded dramatically if the spacing of interdigital electrodes is not small enough.[17,18] Accordingly, the electrode spacing has to be maintained as small as possible, and so a considerable portion of incident photons is blocked by the interdigital electrodes. As a result, the aperture ratio of β-Ga_2O_3 MSM photoconductor is only 50% in general,[17,18] producing a big loss in detection efficiency. Back-illumination mode could be an effective solution to avoid this issue. Nevertheless, incident photons have to pass through the substrate and most of the epilayer before reaching the active layer, and so optimization of device structure (e.g. building a hetero-structure in which a larger-bandgap epilayer is grown on the substrate before the active layer) is required,[1] leading to a significant increase in the difficulty of device fabrication.

Recently, Wan et al reported a Si-based magnetoresistance device with a simple four-terminal structure which presented excellent low-magnetic-field sensing properties comparable with giant-magnetoresistance devices.[19] It is believed improved DUV sensing properties can also be expected for the β-Ga_2O_3 photoconductor by using a similar device structure. Therefore, in this work, a four-terminal photoconductor based on β-Ga_2O_3 epitaxial thin film is proposed as a solar-blind DUV photodetector. Moreover, it is found that its detection sensitivity can be significantly enhanced with the assistance of Zener diodes. Lastly, the device has an aperture ratio over 80%, nearly doubling that of the conventional interdigital MSM devices such as photoconductors and Schottky-type photodiodes.

II. EXPERIMENTAL DETAILS

Firstly, a 100-nm Ga_2O_3 thin film was grown on *c*-plane sapphire substrate by plasma-assisted molecular beam epitaxy (MBE) with Knudsen-cell temperature, substrate-heater temperature, input radio-frequency (RF) power and O_2 flow rate set at 940 °C, 760 °C, 300 W and 1 sccm, respectively. Secondly, four electrodes composed of 20-nm Ti and 80-nm Al were formed on the Ga_2O_3 thin film by electron beam evaporation and lift-off processing. Accordingly, electrodes (5 μm × 22 μm) were placed at each corner of a 50 μm × 50 μm square as shown in Fig. 1, and their spacings were 40 μm (W) and 6 μm (L). Consequently, the aperture ratio of the proposed device exceeded 80%, and a further increase can be expected by using smaller electrodes. Finally, an annealing was performed at 500 °C in N_2 to reduce the contact resistance of the electrodes. When a constant current (I_{14}) is applied between two electrodes (1 and 4), an electric field is generated in the film, leading to
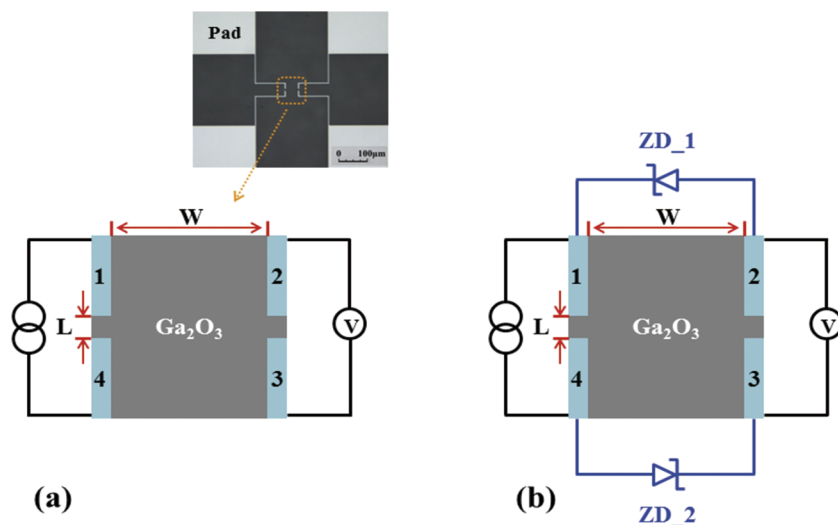

FIG. 1. Device geometry: (a) sample_A, (b) sample_B. The image shows the micrograph of sample_A.

an electric potential difference (U_{23}) between the other two electrodes (2 and 3). Accordingly, electrodes 1 and 4 were connected to an Agilent 4155B to provide the input current, while the other two were connected to a Keithley 2400 for detection of the output voltage. Compared with sample_A, sample_B has two extra reverse-biased Zener diodes (ZD_1 and ZD_2) with same Zener voltage (U_z) of 22 V connected between the electrodes along the W direction. The structural and optical properties of the Ga_2O_3 thin film were investigated by X-ray diffraction (XRD) and UV-visible transmission spectroscopy respectively. In addition, a low-pressure mercury lamp combined with a 254-nm filter acted as the DUV light source during sensing evaluation, and the radiation intensity was calibrated by a UV-enhanced Si photodiode.

III. RESULTS AND DISCUSSIONS

FIG. 2(a) exhibits the out-of-plane XRD spectrum of the Ga_2O_3 thin film grown in this work. It shows that the peaks corresponding to β-Ga_2O_3 ($\bar{2}01$) and its higher-order diffractions were dominant,[3,17] which can be ascribed to the high similarity of oxygen atom arrangement between β-Ga_2O_3 ($\bar{2}01$) plane and sapphire *c*-plane.[20] However, the diffraction peak indexed to β-Ga_2O_3 (400) plane was also observed, indicating a polycrystalline growth. In addition, the optical transmittance spectrum of β-Ga_2O_3 thin film was investigated as presented in FIG. 2(b). A high transmittance of over 80% in visible and near-UV spectral regions together with a sharp cutoff at 270 nm was observed. As shown in the inset of FIG. 2(b), the E_g of the β-Ga_2O_3 thin film was estimated to be 5.0 eV based on Tauc law,[17] and thus its suitability for solar-blind DUV detection was proved.
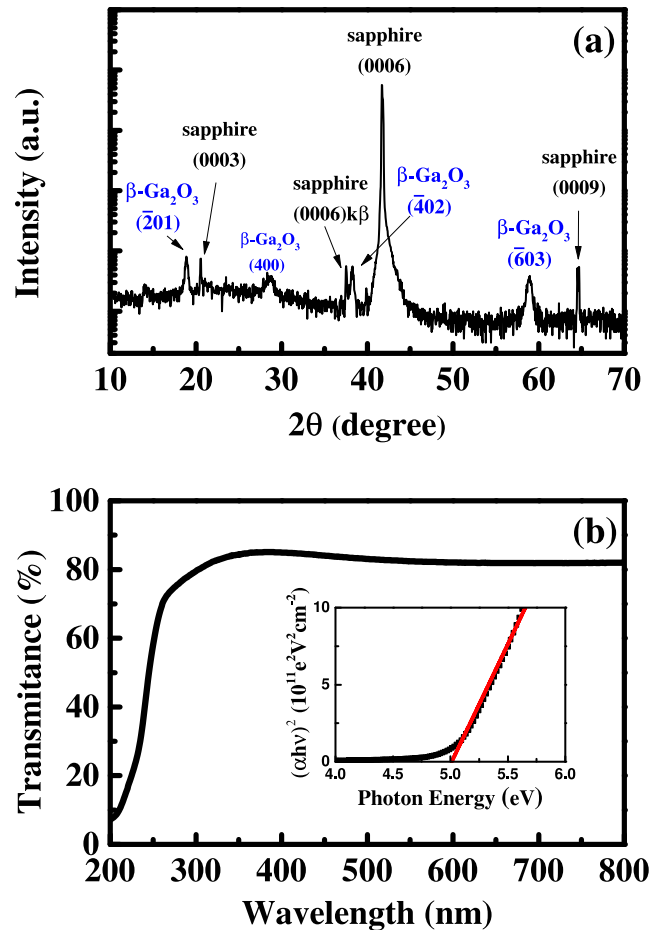

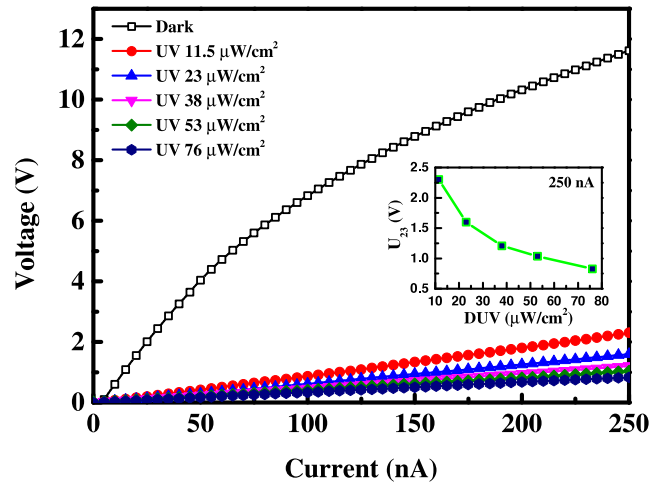FIG. 2. (a) XRD, (b) transmission spectra of the Ga_2O_3 thin film.

FIG. 3. The V-I characteristics of sample_A in dark and under DUV radiation.

As shown in FIG. 3, the voltage-current (V-I) characteristics of sample_A are investigated in dark and under the 254-nm radiation with different power densities. For each radiation condition, U_{23} increases monotonically with increasing I_{14} because a stronger electric field is generated in the film. For a fixed I_{14}, U_{23} drops significantly once a 254-nm radiation is applied, which is more obvious for higher radiation intensity. This phenomenon can be attributed to the following two factors. Firstly, charge carriers are generated in the β-Ga_2O_3 thin film by the radiation, leading to a decrease of film resistivity. Thus, the resistance between the electrodes 2 and 3 (R_{23}) is reduced, which is more significant for stronger radiation. Secondly, under a constant input current I_{14}, I_{23} remains unchanged. Therefore, the radiation-induced lower resistivity of the film results in a reduction of U_{23} (ΔU_{23}), and the reduction extent is related to the radiation intensity. In other words, the DUV radiation can be identified both qualitatively and quantitatively as exhibited in the inset of Fig. 3. For an I_{14} of 250 nA, U_{23} drops from 11.6 V to 0.8 V when the ambient changes from dark to radiation at 76 $\mu W/cm^2$, resulting in a dark/photo voltage ratio of 15.0. This value is comparable to that of previously-reported β-Ga_2O_3 interdigital MSM photoconductor, whose photo/dark current ratio was 11.4.[17]

FIG. 4 exhibits the V-I characteristics of sample_B in dark and under 76-$\mu W/cm^2$ radiation. While the photo voltages of the two samples follow almost the same trend, the dark voltage of
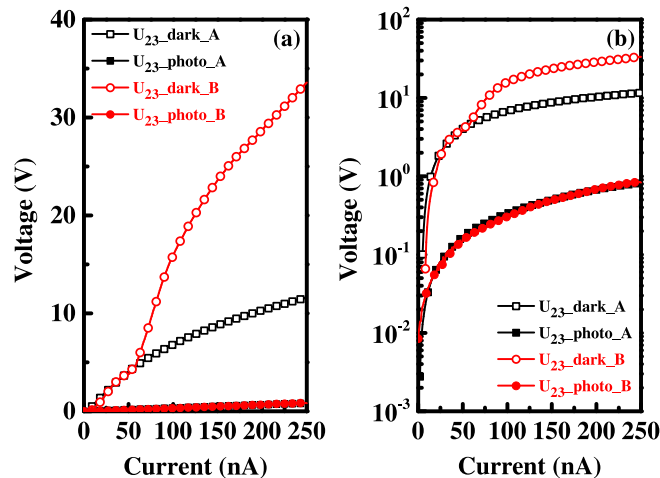

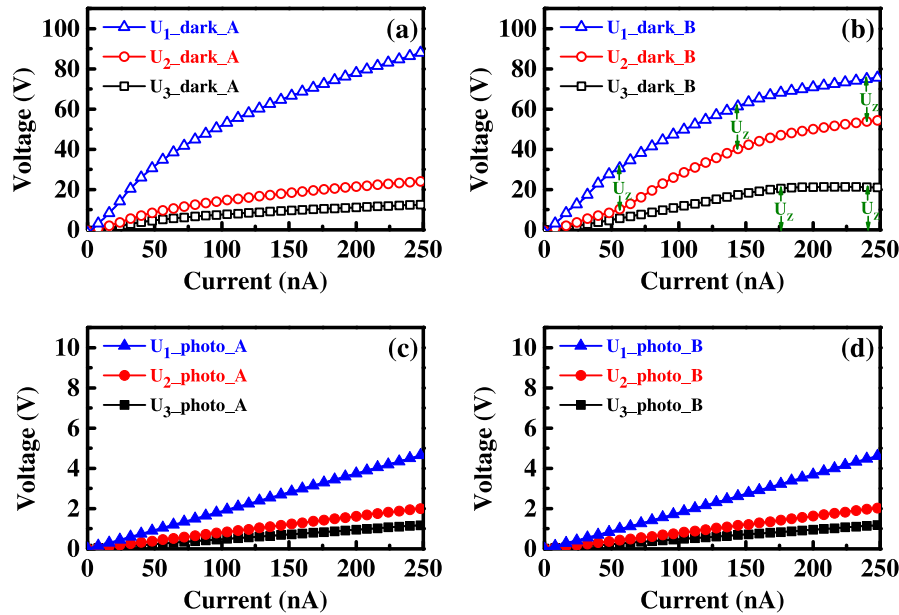FIG. 4. The V-I characteristics of sample_B in dark and under DUV radiation in (a) linear and (b) logarithmic scales.

FIG. 5. Electric potentials of electrodes 1, 2 and 3 versus I_{14}: (a) sample_A in dark; (b) sample_B in dark; (c) sample_A under DUV radiation; (d) sample_B under DUV radiation.

sample_B ($U_{23\_dark\_B}$), compared with that of sample_A ($U_{23\_dark\_A}$), increases more rapidly for I_{14} exceeding ~55 nA, leading to a substantial enhancement in ΔU_{23}. Accordingly, the dark/photo voltage ratio is remarkably increased, which is beneficial to improving the detection sensitivity. For example, for an I_{14} of 250 nA, $U_{23\_dark\_B}$ is increased to 33.6 V, compared to 11.6 V for $U_{23\_dark\_A}$. Under 76-μW/cm^2 radiation, their photo voltages are both 0.8 V, and thus the dark/photo voltage ratio of sample_B is 42, almost treble that of sample_A.

In order to reveal the working mechanism, the electric potentials of electrodes 1, 2 and 3 for the samples in dark (U_{1_dark}, U_{2_dark} and U_{3_dark}) and under 76-μW/cm^2 radiation (U_{1_photo}, U_{2_photo} and U_{3_photo}) are measured with electrode 4 grounded, as exhibited in FIG. 5. On one hand, $U_{1\_dark\_B}$ follows almost the same trend as $U_{1\_dark\_A}$. Moreover, if I_{14} is over ~55 nA, the difference between U_{1dark_B} and $U_{2\_dark\_B}$ is stabilized at 22 V (the value of U_z) by the Zener breakdown of ZD_1 due to the extremely low dynamic resistance between electrodes 1 and 2. As a result, $U_{2\_dark\_B}$ is increased significantly compared with $U_{2\_dark\_A}$, explaining the abrupt increase of $U_{23\_dark\_B}$ in FIG. 4. Meanwhile, $U_{3\_dark\_B}$ is also increased to some extent in comparison with $U_{3\_dark\_A}$ due to the rise of $U_{2\_dark\_B}$. However, $U_{3\_dark\_B}$ begins to stabilize at 22 V for I_{14} exceeding ~175 nA, which is ascribed to the Zener breakdown of ZD_2. Consequently, $U_{23\_dark\_B}$ is further increased. In other words, it is the Zener breakdown of ZD_1 and ZD_2 that induces the substantial increase of $U_{23\_dark\_B}$. This effect can be further enhanced by higher I_{14} and/or smaller U_z for ZD_1 and ZD_2. Moreover, the U_z values of ZD_1 and ZD_2 can be different. On the other hand, there is almost no difference between sample_A and sample_B in U_{1_photo}, U_{2_photo} and U_{3_photo}, leading to nearly the same U_{23_photo} for the two samples, which is consistent with that revealed in FIG. 4. It is due to the fact that either $U_{3\_photo\_B}$ or the difference between $U_{1\_photo\_B}$ and $U_{2\_photo\_B}$ is too small to trigger the Zener breakdown of ZD_2 or ZD_1, and so both Zener diodes act as open circuit, making no impact on the whole detection system. Eventually, the dark/photo voltage ratio of the four-terminal photoconductor is further enhanced.

IV. CONCLUSION

In summary, a β-Ga$_2$O$_3$ solar-blind DUV photodetector based on four-terminal structure and voltage-current operation mode has been proposed and demonstrated. Accordingly, a dark/photo

voltage ratio of 15.0 was achieved, which is sensitive enough to accurately identify the DUV radiation. More importantly, the aperture ratio of our proposed device can be almost double that of the conventional interdigital MSM devices owing to greatly simplified electrode layout, benefiting the detection efficiency. Furthermore, it was found the dark/photo voltage was nearly trebled with the assistance of Zener diodes, providing an effective approach to further improve the detection sensitivity. Hence, this work suggests a promising device for solar-blind DUV detection, especially considering miniaturization, integration and mass production.

ACKNOWLEDGEMENTS

[1] M. Razeghi, P. IEEE **90**, 1006 (2002).
[2] L. W. Sang, M. Y. Liao, and M. Sumiya, Sensors **13**, 10482 (2013).
[3] D. Y. Guo, Z. P. Wu, Y. H. An, X. C. Guo, X. L. Chu, C. L. Sun, L. H. Li, P. G. Li, and W. H. Tang, Appl. Phys. Lett. **105**, 023507 (2014).
[4] R. Suzuki, S. Nakagomi, Y. Kokubun, N. Arai, and S. Ohira, Appl. Phys. Lett. **94**, 222102 (2009).
[5] W. Y. Weng, T. J. Hsueh, S. J. Chang, G. J. Huang, and H. T. Hsueh, IEEE Sens. J. **11**, 999 (2011).
[6] M. Razeghi and A. Rogalski, J. Appl. Phys. **79**, 7433 (1996).
[7] S. Ghanbarzadeh, S. Abbaszadeh, and K. S. Karim, IEEE Electron Device Lett. **35**, 235 (2014).
[8] A. Khosropour and A. Sazonov, IEEE Electron Device Lett. **35**, 768 (2014).
[9] R. Suzuki, S. Nakagomi, and Y. Kokubun, Appl. Phys. Lett. **98**, 131114 (2011).
[10] M. Orita, H. Ohta, M. Hirano, and H. Hosono, Appl. Phys. Lett. **77**, 4166 (2000).
[11] V. Kuryatkov, A. Chandolu, B. Borisov, G. Kipshidze, K. Zhu, S. Nikishin, H. Temkin, and M. Holtz, Appl. Phys. Lett. **82**, 1323 (2003).
[12] Y. Z. Chiou, Y. C. Lin, and C. K. Wang, IEEE Electron Device Lett. **28**, 264 (2007).
[13] Z. G. Ju, C. X. Shan, D. Y. Jiang, J. Y. Zhang, B. Yao, D. X. Zhao, D. Z. Shen, and X. W. Fan, Appl. Phys. Lett. **93**, 173505 (2008).
[14] T. Oshima, T. Okuno, N. Arai, N. Suzuki, S. Ohira, and S. Fujita, Appl. Phys. Express **1**, 011202 (2008).
[15] P Feng, J. Y. Zhang, Q. H. Li, and T. H. Wang, Appl. Phys. Lett. **88**, 153107 (2006).
[16] S. Nakagomi, T. Momo, S. Takahashi, and Y. Kokubun, Appl. Phys. Lett. **103**, 072105 (2013).
[17] D. Y. Guo, Z. P. Wu, P. G. Li, Y. H. An, H. Liu, X. C. Guo, H. Yan, G. F. Wang, C. L. Sun, L. H. Li, and W. H. Tang, Opt. Mater. Express **4**, 1067 (2014).
[18] T. Oshima, T. Okuno, and S. Fujita, Jpn. J. Appl. Phys. **46**, 7217 (2007).
[19] C. H. Wan, X. Z. Zhang, X. L. Gao, J. M. Wang, and X. Y. Tan, Nature **477**, 304 (2011).
[20] S. Nakagomi and Y. Kokubun, J. Cryst. Growth **349**, 12 (2012).